7.4 A VARIATIONAL FORMULATION OF THE VOLTERRA DISLOCATION RECONSTRUCTION OF 3-D MOVING CRACKS—A. Sheng, G. Po, N.M. Ghoniem (University of California, Los Angeles)

OJBECTIVE

The evolution equations governing a Volterra dislocation-based reconstruction of moving 3-D cracks are formulated using a variational approach based on the Principal of Maximum Entropy Production rate (PMEP).

SUMMARY

Modeling crack growth in three-dimensional geometries poses a challenging problem especially for FEM-based techniques such as EFEM or XFEM, which display some degree of mesh dependence. Additionally, existing methods are unable to investigate the interaction between cracks and other defects present in real materials. An alternative method developed in the framework of discrete Dislocation Dynamics is presented which provides a solution to these challenges by being completely mesh-independent and capable of coupling cracking with crystal plasticity. The Discrete Crack Mechanics method is a dislocation-based fracture mechanics technique that represents cracks using arrays of Volterra dislocations. In this report, a variational formulation based on the Principle of Maximum Entropy Production rate is given of the evolution equations for cracks coupled with crystal dislocations along with examples of its implementation.

PROGRESS AND STATUS

Introduction

The resemblance between the elastic fields of cracks and dislocation arrays has long been recognized and is the foundation for the Discrete Crack Mechanics (DCM) method outlined in this report [1, 2]. In DCM, cracks are represented by arrays of discrete Volterra dislocations that are henceforth referred to as crack dislocations in order to distinguish them from crystal dislocations. DCM is an extension of the discrete Dislocation Dynamics (DD) method originally developed to investigate the evolution of crystal dislocation patterns [3, 4, 5]. In DD, dislocations are represented by parametric space curves and their interactions in 3-D are completely resolved. In DCM, crack dislocations are represented in the same manner allowing us to not only model cracks with complex shapes but also capture interactions between multiple cracks as well as between cracks and crystal dislocations.

Crack propagation occurs when the J-integral, or equivalently, the stress intensity factor K of a crack exceeds a critical value unique to the material. The J-integral, which can be shown to be equivalent to the unbalanced PK force on the leading dislocation in DCM, is what drives the motion of the crack tip. In this report, we present a variational formulation of the evolution equations for a system containing cracks as well as crystal dislocations. This approach utilizes the Principal of Maximum Entropy Production Rate (PMEP) to find the equations governing the motion of cracks and crystal dislocations, which are considered irreversible fluxes contributing to the internal entropy production of the system.

Dislocation-Based Fracture Mechanics

A loaded crack is completely described by a distribution of crack dislocation loops with suitable Burger's vectors $\boldsymbol{b}$. The crack tip loop, or leading dislocation, is fixed and determines the size and shape of the crack. Enclosed by this loop is a series of additional loops referred to as trailing dislocations which, as a result of the applied load, their mutual interactions, and their interactions with the crack-tip loop, experience a configurational force known as the Peach-Koehler (PK) force. When tractions are applied to an elastic body, forces cannot be transferred across crack surfaces, which remain traction-free. This condition is satisfied when the PK forces on the trailing crack dislocations are balanced. The leading dislocation however, experiences an unbalanced PK force that drives crack growth if the corresponding K

exceeds the fracture toughness of the material K_C. The equations governing the motion of crack tips and crystal dislocations are derived in the following section.

Quasi-Static Crack Motion

The Principal of Maximum Rate of Entropy Production, or PMEP, states that generalized fluxes in an evolving system maximize the internal entropy production rate. In continuum mechanics, the expression of the second law of thermodynamics is referred to as the Clausius-Duhem statement [5]. For a body Ω with no sources of internal entropy production other than cracks and crystal dislocations, the Clausius-Duhem statement is given by:

$$-\rho_0\dot{\psi} + \sigma_{kj}v_{j,k} = \theta\pi \ \geq 0 \tag{1}$$

where ρ_0 is the mass density per unit volume, ψ the Helmholtz free energy density, σ_{jk} the Cauchy stress tensor, $v_{j,k}$ the distortion rate, θ the absolute temperature, and π the rate of internal entropy production. The distortion rate may be written in terms of the elastic distortion tensor β_{ij}^E, the plastic distortion tensor β_{ij}^P, and the crack distortion tensor β_{ij}^C by:

$$v_{i,j} = \ \dot{\beta}_{ij}^E + \dot{\beta}_{ij}^P + \dot{\beta}_{ij}^C \tag{2}$$

The plastic distortion tensor is given by [6]:

$$\beta_{ij}^P = \int_{S^P} b_i^P \delta(\boldsymbol{x} - \boldsymbol{x}')da_j' \tag{3}$$

where $S^P$the surface is bounded by the crystal dislocation loop and b_i^p is the crystal dislocation Burger's vector. Similarly, the crack distortion tensor is given by:

$$\beta_{ij}^C = \int_{S^C} b_i^C(\boldsymbol{x}')\delta(\boldsymbol{x} - \boldsymbol{x}')da_j' \tag{4}$$

where $S^C$the surface is bounded by the crack tip dislocation loop and $b_i^C(\boldsymbol{x}')$ is the crack dislocation Burger's vector, which is a function of the position $\boldsymbol{x}'$ on the crack plane. If the Helmholtz free energy density ψ is taken to be of the form:

$$\psi \equiv \psi(\boldsymbol{\beta^E}, \boldsymbol{\beta^P}) \tag{5}$$

then its material time derivative is given by:

$$\dot{\psi} = \frac{\partial\psi}{\partial\beta_{ij}^E}\dot{\beta}_{ij}^E + \frac{\partial\psi}{\partial\beta_{ij}^P}\dot{\beta}_{ij}^P \tag{6}$$

Substituting equations 2 and 6 into equation 1 and combining like terms gives:

$$\left(-\rho_0\frac{\partial\psi}{\partial\beta_{ij}^E} + \sigma_{ij}\right)\dot{\beta}_{ij}^E + \left(-\rho_0\frac{\partial\psi}{\partial\beta_{ij}^P} + \sigma_{ij}\right)\dot{\beta}_{ij}^P + \sigma_{ij}\dot{\beta}_{ij}^C = \theta\pi \geq 0 \tag{7}$$

Since elastic deformation is recoverable, it does not contribute to the internal entropy production rate and thus the first term in equation 7 gives the constitutive relation:

$$\sigma_{ij} = \rho_0\left.\frac{\partial\psi}{\partial\beta_{ij}^E}\right|_{\beta^P} \tag{8}$$

In the second term is a stress-like quantity, $\tau_{ij} = \rho_0 \frac{\partial \psi}{\partial \beta_{ij}^P}$, represents a change in the lattice energy due to a change in local plastic deformation. Using this definition, the Clausius-Duhem statement may be rewritten as the products of generalized forces and fluxes:

$$\frac{1}{\theta}\left(\sigma_{ij} - \tau_{ij}\right)\dot{\beta}_{ij}^P + \frac{\sigma_{ij}}{\theta}\dot{\beta}_{ij}^C = \pi \geq 0 \tag{9}$$

For convenience in the followings steps we use the following definition for the L.H.S. of equation (9), which contains all of the contributions to the internal entropy production rate:

$$\varphi \equiv \frac{1}{\theta}\left(\sigma_{ij} - \tau_{ij}\right)\dot{\beta}_{ij}^P + \frac{\sigma_{ij}}{\theta}\dot{\beta}_{ij}^C \tag{10}$$

While equation 9 constrains π to be the product of the generalized forces and fluxes, alone it is insufficient for determining the evolution equations for the system. To obtain the evolution equations, we must combine PMEP and equation 10 to formulate a constrained functional for π using the method of Lagrange multipliers:

$$\Pi = \int_\Omega [\pi + \lambda(\pi - \varphi)]\, dV \tag{11}$$

It can be shown that the value of the Lagrange multiplier λ is determined by $\lambda = n/(1-n)$ where n is the order of π in the generalized fluxes. Taking π to be a quadratic functional of the irreversible general fluxes $\boldsymbol{w^P}$ and $\boldsymbol{w^C}$, which are the dislocation velocity and crack tip velocity respectively, one obtains:

$$\pi[\boldsymbol{w^P}, \boldsymbol{w^C}] = \oint_{L^P} \delta(\boldsymbol{x} - \boldsymbol{x}')B_{ij}^P w_i^P w_j^P dl' + \oint_{L^C} \delta(\boldsymbol{x} - \boldsymbol{x}')B_{ij}^C w_i^C w_j^C dl' \tag{12}$$

The first term corresponds to the energy dissipated by motion of the dislocation loop L^P, while the second term is associated with the energy dissipated by motion of the crack tip loop L^C during crack growth. Substituting equations 10 and 12 as well as the Lagrange multiplier value $\lambda = -2$ into equation 11 gives:

$$\Pi = \int_\Omega \left[\frac{2}{\theta}\left(\sigma_{ij} - \tau_{ij}\right)\dot{\beta}_{ij}^P + \frac{2\sigma_{ij}}{\theta}\dot{\beta}_{ij}^C - \oint_{L^P} \delta(\boldsymbol{x} - \boldsymbol{x}')B_{ij}^P w_i^P w_j^P dl' - \oint_{L^C} \delta(\boldsymbol{x} - \boldsymbol{x}')B_{ij}^C w_i^C w_j^C dl'\right] dV \tag{13}$$

Taking the material time derivatives of equations 3 and 4 give the plastic and crack distortion rates to be:

$$\dot{\beta}_{ij}^P = \oint_{L^P} \delta(\boldsymbol{x} - \boldsymbol{x}')b_i^P \epsilon_{jkm} w_k^P dl'_m \tag{14}$$

$$\dot{\beta}_{ij}^C = \oint_{L^C} \delta(\boldsymbol{x} - \boldsymbol{x}')b_i^C(\boldsymbol{x}')\epsilon_{jkm} w_k^C dl'_m + \int_{S^C} \dot{b}_i^C(\boldsymbol{x}')\delta(\boldsymbol{x} - \boldsymbol{x}')da'_j \tag{15}$$

Substituting equations 14 and 15 into 13 and utilizing the sifting property of the Dirac δ function, Π may be written as a functional of the irreversible generalized fluxes $\boldsymbol{w^P}$, $\boldsymbol{w^C}$, and $\dot{\boldsymbol{b}}^C$ which can be thought of as a "crack opening displacement flux":

$$\begin{aligned}\Pi\left[\boldsymbol{w^P}, \boldsymbol{w^C}, \dot{\boldsymbol{b}}^C\right] = \int_{\boldsymbol{S^C}} \frac{2\sigma_{ij}}{\theta}\dot{b}_{\boldsymbol{i}}^{\boldsymbol{C}} n_j da + \oint_{L^C}\left[\frac{2\sigma_{ij}}{\theta}\left(b_i^C(\boldsymbol{x}')\epsilon_{jkm} w_k^C \hat{\xi}_m\right) - B_{\boldsymbol{ij}}^{\boldsymbol{C}} w_{\boldsymbol{i}}^{\boldsymbol{C}} w_{\boldsymbol{j}}^{\boldsymbol{C}}\right] dl \\ + \oint_{L^P}\left[\frac{2}{\theta}\left(\sigma_{ij} - \tau_{ij}\right)b_i^P \epsilon_{jkm} w_k^P \hat{\xi}_m - B_{ij}^P w_i^P w_j^P\right] dl\end{aligned} \tag{16}$$

By taking the variation of Π with respect to its arguments and imposing stationarity:

$$\begin{aligned}\delta\Pi = \int_{S^C}\left(\frac{\sigma_{ij}}{\theta}n_j\right)\delta\dot{b}_i^C da + \oint_{L^C}\left(\frac{1}{\theta}\epsilon_{ijk}\sigma_{jm} b_m^C \hat{\xi}_k - B_{ij}^C w_j^C\right)\delta w_i^C dl \\ + \oint_{L^P}\left[\frac{1}{\theta}\epsilon_{ijk}\left(\sigma_{jm} - \tau_{jm}\right)b_m^P \hat{\xi}_k - B_{ij}^P w_j^P\right]\delta w_i^P dl = 0\end{aligned} \tag{17}$$

one obtains the equations of motion governing the evolution of the system. From the third term comes the celebrated Peach-Koehler force per unit dislocation length: $\epsilon_{ijk}\sigma_{jm}b_m^p\hat{\xi}_k$ and the lattice force per unit dislocation length: $\epsilon_{ijk}\tau_{jm}b_m^p\hat{\xi}_k$. The first and second terms give the governing equations for crack motion. The first term requires that the crack surface remain traction free, as discussed in the previous section:

$$\sigma_{ij}n_j = 0 \quad \text{on crack surface } S^C \tag{18}$$

The second term indicates that the crack tip velocity is proportional to the unbalanced PK force acting on it, mimicking the motion of a crystal dislocation:

$$\frac{1}{\theta}\epsilon_{ijk}\sigma_{jm}b_m^C\hat{\xi}_k = B_{ij}^C w_j^C \tag{19}$$

Implementation and Examples

The procedure for simulating crack growth is described as follows:

1. A leading dislocation loop corresponding to the shape of the crack is inserted into the body to which a prescribed load or displacement is applied.
2. Trailing dislocation loops are inserted and allowed to equilibrate according to the PK force acting on them.
3. If the *K* calculated along the leading dislocation is found to be below the fracture toughness K_C, the crack is static and the simulation is terminated.
4. If *K* at any segment along the leading crack dislocation exceeds K_C , the loop is advanced according to equation 19.
5. Steps 2-3 are repeated until *K* no longer exceeds K_C or the body is fractured completely.

Three examples in which DCM is used to model crack growth are provided below. The first example shows the growth of a penny-shaped crack in a cylinder to which a constant traction is applied as shown in Figure 1a. The second example is the growth of a penny-shaped crack in a cylinder to which a fixed displacement is applied as shown in Figure 1b.

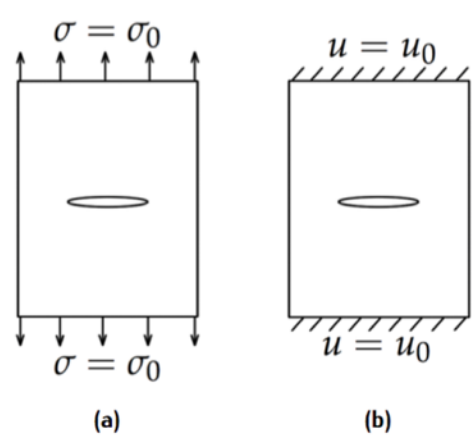

Figure 1. (a) Constant stress "dead-load" loading **(b)** Fixed displacement "fixed-grips" loading.

In the third example, a penny-shaped crack in a rectangular pillar is shown to grow preferentially towards the closest boundaries due to the increased boundary effect. The material used in all three examples has a shear modulus of G = 18.5 GPa, a Poisson's ratio of v = 0.27, and a fracture toughness of K_C = 2.5 MPa-m$^{1/2}$.

Crack Growth Under Constant Applied Stress

In this example, a constant traction is applied to the upper and lower surfaces of a cylinder with a height of h = 8 mm and a radius of r_0 = 4 mm. The cylinder contains a penny-shaped crack with an initial radius of r = 400 μm. As shown in Figure 2, the stress intensity factor of the crack increases as the crack propagates.

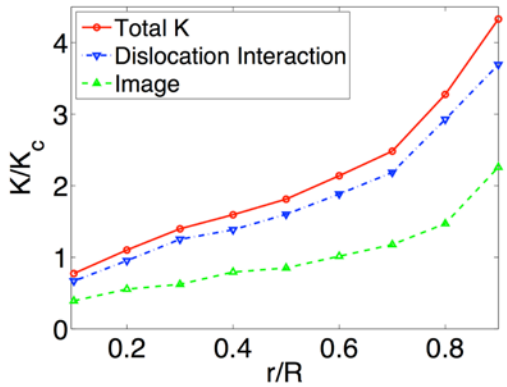

Figure 2. K/K_C vs. r/r_0 curve showing the increase in K/K_C as the crack grows under dead-load conditions.

Crack Growth Under Fixed Displacement

In the second example, a fixed displacement of 10 μm is applied to the upper and lower surfaces of a cylinder with a height of h = 8 mm and a radius of r_0 = 4 mm. A penny-shaped crack with an initial radius of r = 400 μm is placed in the center of the cylinder. Figure 3 shows that the stress intensity factor of the crack increases as the crack propagates but at a lower rate than the crack under a dead load. This is due to the fact that under fixed-grip conditions, the material relaxes and essentially becomes more compliant as the crack grows.

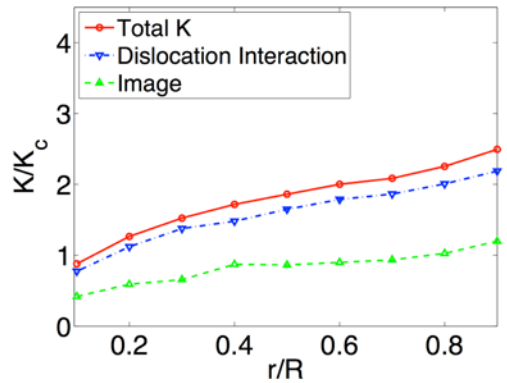

Figure 3. K/K_C vs. r/r_0 curve showing the increase in K/K_C as the crack grows under fixed-grip conditions.

Preferential Crack Growth Due to Boundary Effects

In the third example, a rectangular pillar with a height of h = 4 mm, a width of w = 2.5 mm, and a thickness of t = 1 mm contains a penny-shaped crack at its center with an initial radius of r_0 = 0.25 mm as shown in Figure 4. A constant traction of 155 MPa is applied to the top and bottom surfaces of the pillar.

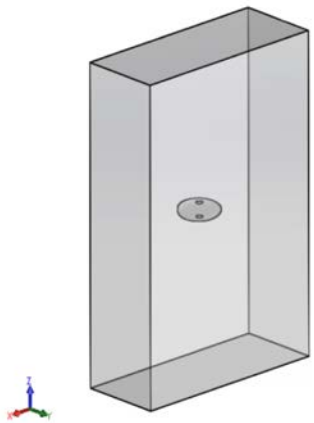

Figure 4. Rectangular pillar with a penny-shaped crack at its center.

The crack edges closest to the free boundaries of the pillar propagate at a faster rate than the edges that are further from the free boundaries as shown in Figure 5. This is because of the fact that the crack edges nearer to the free boundaries experience larger PK forces due to an increased boundary effect. The result is an elongation of the initially circular crack into an elliptical shape as it propagates. Note that the crack opening displacement also increases since more loops are required to achieve an equilibrium configuration as the crack increases in size.

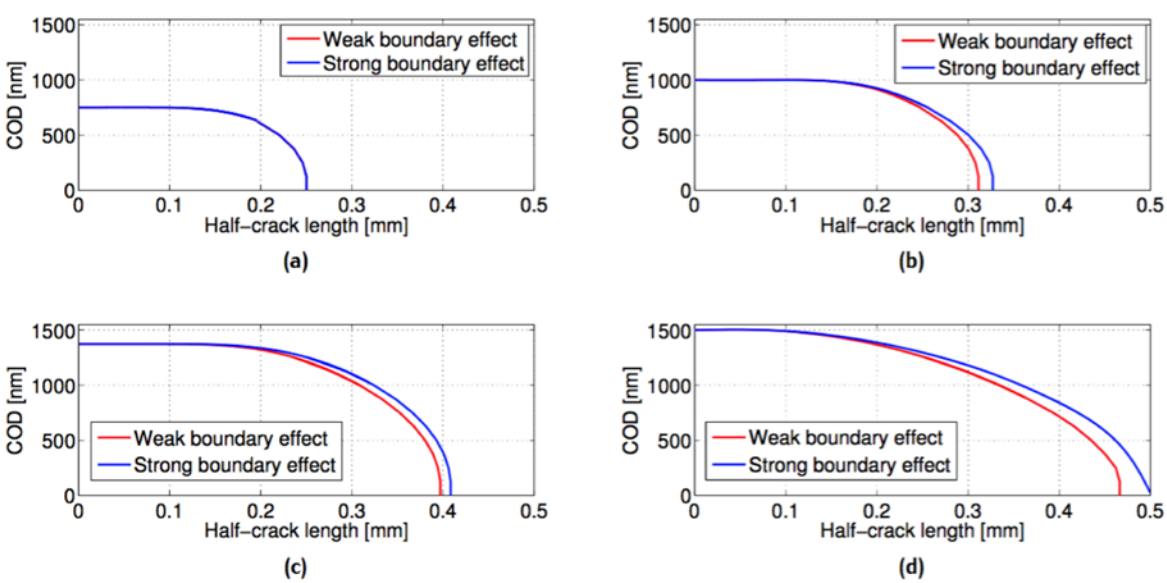

Figure 5. Crack profile along the major and minor axes of the pillar at **(a)** 822 simulation steps, **(b)** 2057 simulation steps, **(c)** 4515 simulation steps, **(d)** 4956 simulation steps (complete fracture).

References

[1] J. D. Eshelby, F. C. Frank, and F. R. N. Nabarro, *The London, Edinburgh, and Dublin Philosophical Magazine and Journal of Science*, **42 (327)** (1951), 351.
[2] J. Weertman, in Dislocation Based Fracture Mechanics, *World Scientific*, 1996, 33.
[3] N. M. Ghoniem and R. J. Amodeo, *Solid State Phenomena* **3&4** (1988)**,** 377-388.
[4] E. van der Giessen and A. Needleman, *Modelling Simul. Mater. Sci. Eng.* **3** (1995), 689.
[5] G. Po and N.M. Ghoniem, *JMPS* **66** (2014), 103.
[6] T. Mura, in Micromechanics of Defects in Solids, *Martinus Nijhoff Publishers*, 1987, 50-53.